Chapter

In Situ Detection of Leakages in Partition Elements through SONAH and Beamforming Techniques

José A. Ballesteros, Samuel Quintana and Marcos D. Fernandez

Abstract

Airborne sound insulation in buildings, whether in fixed partition elements, like partitions or party walls, or mobile elements, like doors or screens, is always related to the performance of the weakest element involved. In situ assessment of airborne sound insulation in building elements can be carried out by pressure techniques or sound intensity techniques. Sound pressure techniques are very quick but fail to discriminate the sound insulation contribution of each building element involved. Sound intensity techniques, on the other hand, allow to determine the sound transmission of each element and also to discriminate indirect transmissions up to a certain degree. In order to find areas with high sound transmission, such as leakages or weakened regions, a large number of measurements on the building element surface have to be performed. Moreover, the sound intensity technique is very time-consuming, because it is necessary to carry out the measurement in each grid point defined. This chapter describes the use of beamforming and SONAH techniques to detect areas with lower airborne sound insulation in a building element. These techniques unify the advantages of both, pressure and sound intensity techniques, allowing the quick visualization of leakages or weakened areas of different building elements.

Keywords: building, insulation, leakage, SONAH, beamforming

1. Introduction

Standard in situ methods to obtain airborne sound insulation in building elements are based on sound pressure measurements (ISO 16283-1) [1] and on sound intensity measurements (ISO 15186-2) [2].

The method described in ISO 16283-1 [1] states that the acoustic field generated at the emitting room must be diffuse, stationary, and spectrally flat, at least for the frequency range under consideration (100–3150 Hz). Acoustic field and reverberation time measurements are averaged in space and time to ensure low statistical spread.

The apparent sound reduction index (R') is one of the parameters used to express the acoustic behavior, and it stems from Eq. (1):

$$R'\,[dB] \;=\; \overline{L_1} - \overline{L_2} + 10\log\frac{S}{A} \tag{1}$$

$$A[m^2] \;=\; \frac{0.16V}{T} \tag{2}$$

where

- $\overline{L_1}$ [dB] is the average sound pressure level at the emitting room.
- $\overline{L_2}$ [dB] is the average sound pressure level at the receiving room.
- S [m^2] is the total surface of the common partition element between both rooms.
- A [m^2] is the equivalent acoustic absorption area at the receiving room. It is obtained using the Sabine Eq. (2).
- V [m^3] is the volume of the receiving room.
- T [s] is the reverberation time in the receiving room.

The main difference in the measurement procedure ISO-15186-2 [2] regarding to ISO 16283-1 [1] is that reverberation time measurement is not required, and in the receiving room, the measured parameter is the acoustic intensity normal to the surface of the partition element being assessed, whether by scanning or by grid techniques, depending on the resolution required. In this case, the acoustic behavior is defined by the apparent sound reduction index by intensimetry R'_I, which is different from the index obtained by acoustic pressure and is calculated according to Eq. (3):

$$R'_I\,[dB] \;=\; \left[\overline{L_{p1}} - 6 + 10\log\frac{S}{S_0}\right] - \left[\overline{L_{In}} + 10\log\frac{S_M}{S_0}\right] \tag{3}$$

where

- $\overline{L_{p1}}$ [dB] is the average noise pressure level at the emitting room.
- S [m^2] is the surface of the partition element under study.
- $\overline{L_{In}}$ [dB] is the average sound intensity level, normal to the measuring surface/s in the receiving room.
- SM [m^2] is the total surface of the measuring surface/s.
- S0 (1 m^2) is the reference surface.

The procedure described in ISO-15186-2 [2] provides a partial assessment of the sound insulation of each surface present in the partition element. Nevertheless, the final evaluation of the acoustic behavior depends strongly on the resolution defined throughout the measurement procedure and is closely related to a high density of

measuring points. The validity range of this technique is determined through the calculation and the monitoring of the so-called field indicators (F_2, F_3, F_4) according to ISO 9614-1 [3], which allow to ascertain whether the acoustic intensity measurement conditions fulfill or not the minimal requirements.

After the examination of the measurement procedures, it is noticed that the main advantages of the pressure method [1] are its standardization and the reduced time required to take the measurement; its main disadvantages are the incapability of detecting leaks and areas with a poor insulation level, and, additionally, it does not reject the possible indirect transmissions. On the contrary, the technique based on intensity measurements [2], identifies leakages or weakened areas; its resolution, however, depends on the density of points of the measuring grid and hence, on the measuring time for each test. In order to achieve intensity data with high resolution in terms of space and frequency, a highly dense (every 5–10 cm) point grid must be designed, which leads to long measuring times.

A new measurement procedure is proposed to unify the advantages of both methods mentioned above: quickness and detection of leaks. This new procedure is based on beamforming and accompanied by SONAH; its main aim is the identification of the areas with weak insulation in one shot measurement [4].

Beamforming is performed, in its simplest approach, through the delay-and-sum algorithm, which consist of the sum of the delayed signals from the array microphones with different delays in order to put all the signals in phase. With this, the signal of interest is reinforced against the noise and other signals propagating in other directions [5].

In the statistically optimal near-field acoustic holography (SONAH) method [6], the acoustic quantities on a mapping surface near the measurement surface are calculated by using a transfer matrix defined in such a way that all the propagating waves and a weighted set of evanescent waves are projected with optimal average accuracy. The main advantage of SONAH is the fact that it does not use the discrete spatial Fourier transform used in the classical NAH procedure. Therefore, undesirable spatial leakage effects are avoided [7].

SONAH [6] and beamforming [8] techniques use a measurement system based on specially designed geometrical configurations of microphone arrays [9], which help to understand the acoustic field at a given distance from the acoustic source, using various signal processing algorithms. These techniques are mainly used to locate acoustic sources [10].

Besides the different array geometries [11] and algorithms [5] used, the main differences in practical applications between SONAH and beamforming techniques reside in:

- The distance between the array and the acoustic field—SONAH technique requires near-field measurements close to the surface [6], whereas beamforming technique does the measurements in the far field [12].

- In the covered surface of study.

- In the use of references, which are mandatory in SONAH.

Using only one of these two methods—beamforming or SONAH—would not suffice to cover the whole frequency range of interest (100–3150 Hz), since beamforming shows poor resolution in low-frequency range and SONAH requires a large number of microphones to attain good resolutions at high frequency [13]. Therefore, a combination of both methods can be applied throughout the desired range.

2. Methodology

All the recommendations laid down in measurements based on pressure [1] and intensity [2] standards have been interrelated regarding the execution of the beamforming and SONAH measurements.

In the emitting room, two omnidirectional sound sources, one placed close to a corner generating white noise and the other one in the center of the room generating pink noise, are independently triggered and equalized to generate an acoustic field diffuse, stationary, and spectrally flat (90–95 dB approx.) with no tonalities over the desired frequency range.

At the receiving room measurement positions are defined based on the features of the surface under study, the instrumentation, and the technique used.

Beamforming technique states that the measuring distance between the array and the source, to cover the whole area of interest at the partition element, must be the minimum value required according to Eq. (4) [14]:

$$L = 1.15z \tag{4}$$

where

- z [m] is the measuring distance.
- L [m] is the length of the sound source.

Nevertheless, the bigger the distance of Beamforming measurement is, the lower the resolution will be, and therefore, the more difficult will be to locate the maximum sound radiation areas. The resolution can be calculated according to Eq. (5):

$$R = 1.22\left(\frac{z}{D}\right)\lambda \tag{5}$$

where

- R [m] is the resolution.
- $\lambda\,[m] = \frac{c\,\left[\frac{m}{s}\right]}{f\,[Hz]}$ is the wavelength.
- D [m] is the array diameter.

Taking this into account, in the measurements, distances from the partition element should be chosen in such a way that the array can be placed at a distance that allows to fully cover the surface under study, carefully combining the values for calculation distance, covered surface, and expected resolution.

When the measurements have been taken, to process the data, the calculation points are defined over a flat grid. This grid should have an x/y axis spacing as dense as possible in order to allow an accurate identification of leaks, fissures, or sealing defects.

Once defined the calculation grid, the simplest algorithm that can be used is the delay-and-sum one. With this algorithm, it is possible to define the minimum working frequency for a 30° opening angle as [12].

$$f_{min}\left(30^{\circ}\right) = \frac{c}{D} \tag{6}$$

with

- c the speed of sound (344 m/s)
- D [m] the array diameter

The highest frequency is defined according to the sidelobe level as

$$f_{max}\left(30^{\circ}\right) = \frac{4}{3} f_T, \tag{7}$$

being f_T [Hz] the sidelobe threshold frequency [12].

The frequency range obtained can be used for the case of the beamforming delay-and-sum algorithm and could be increased if other algorithms (such as minimum variance or Capon [15], clean-SC [16], DAMAS [17], beamforming through using eigenvalues and eigenvectors [18], MUSIC [19], or orthogonal beamforming [20]) are used.

In the case of SONAH measurements, the instrumentation setup is configured to carry out the measurements in the near field. The calculation grid is limited by the array dimensions (although we can take more measurements to synthesize a larger grid [21]). Depending on the array dimensions and the possibility of synthesizing a large grid, the measurements can be performed in two manners:

- Over the whole partition element
- Over smaller characteristic areas, made with different materials, where there might be suspicions fissures or leakages

The use of references is compulsory in SONAH. They are selected according to the features of the sound field at the receiver (microphone references) [22] or to the vibration level at the partition elements (accelerometer references) [14], which could be related to sound insulation by the pressure and intensity calculations obtained by these techniques.

For SONAH measurements, the working frequency range is determined by

$$f_{min}\,[Hz] = \frac{d}{2D} \tag{8}$$

and

$$f_{max}\,[Hz] = \frac{c}{2dx} \tag{9}$$

where

- c is the speed of sound (344 m/s).
- dx [m] is the average spacing between array microphone positions.
- D [m] is the diameter of the array.

Once the array-based measurements are performed and processed, results are displayed in color maps where the areas of the studied surface with higher pressure

or intensity levels can be identified. These areas, therefore, corresponding to leaks, fissures, or sealing defects, are those with higher sound transmission.

2.1 Practical application of the method

An applied experiment has been carried out to check the correctness, validity, and practicability of this new methodology to quickly detect in situ acoustic leakages.

Specifically, in situ measurements were performed through multiple testing of various partition elements present in different buildings. Partition elements were chosen as a broad sample of the most common elements in use, both by their typology and materials [23]. Eight different partition elements were selected to validate the method, such as laminated plasterboard wall and different kinds of homogeneous or heterogeneous doors made of metal, wood, or glass. The assessment of those doors considered their placement onto either a plasterboard system partition element or a normal brick wall, with better sound insulation properties than the door itself; in all cases, walls with minimum indirect transmission conditions were selected (i.e., surrounding walls with heavy elements and T junctions, without ventilation grids nor cabling boxes) [24]. **Figure 1** displays all the partition elements under study. **Table 1** summarizes the main features of the performed tests, where

- *Ve* [m^3] and *Vr* [m^3] are the volume of emitting and receiving rooms, respectively.
- *Sse* [m^2] and *Ssr* [m^2] are the floor surface of emitting and receiving rooms, respectively.
- *ST* [m^2] is the total surface of partition element or common compartmentalization element.

To perform beamforming and SONAH measurements, an 18-microphone slice wheel array (**Figure 2**) was used. Ten-second time signals were recorded with the array linked to a data acquisition system with a sample frequency of 65,536 Hz [25] governed by a computer.

In the beamforming measurements performed, the distances varied between 2 and 5 m from the partition element. **Figure 3** shows the beamforming layout used to carry out the measurements.

To process the data, the delay-and-sum algorithm was used over a flat grid with a maximum x/y axis spacing of 0.05 m. With this algorithm and an array diameter of 35 cm, the minimum working frequency would be about 1 kHz, according to Eq. (6). Moreover, defining a threshold $T = -8\,dB$, as it is established by the manufacturer of the array for the delay-and-sum algorithm, and taking into account the array characteristics, applying Eq. (7), a $f_{max}(30°)$ about 6143 Hz is obtained [26]. Taking this into account, the frequency range was defined from the third octave band centered on 1 kHz to the one centered on 5 kHz.

In SONAH measurements, since the array is 35 cm in diameter, they were performed at a distance on 10 cm on areas where fissures could be observed, which can be those characteristic areas of the door made with different materials or because they had some particularities. **Figure 4** shows the SONAH layout used to carry out the measurements.

To process the data, a flat grid with a maximum x/y axis spacing of 0.01 m was used. As the average spacing between measurement points is 0.073 m and D is 0.35 m, and applying Eqs. (8) and (9), the minimum working frequency would

Figure 1.
Photographs of partition elements under study (descriptions of each Id. included in ***Table 1****).*

be 123 Hz and the maximum working frequency 2353 Hz [26]. Taking this into account, the measurements were taken from the third octave band centered on 160 Hz to the one centered on 1600 Hz.

Both beamforming and SONAH tests were post-processed considering also the option of including reference signals. In this way, five reference signals were used: two vibrating signals and three sound pressure signals. Since some partition elements are made of two different materials, it was decided to place an accelerometer centered on the surface of each material and three microphones in the array plane along a diagonal line across the assessed surface [27]: top left, center, and bottom right. **Figures 3** and **4** show the reference configuration in each case.

Id.	Description	Emitter		Receiver		Surface	R'_w [dB] ISO 16283-1
		Ve [m^3]	*Sse* [m^2]	*Vr* [m^3]	*Ssr* [m^2]	*ST* [m^2]	
1	Plasterboard wall	519	181	219	75	16.7	35
2	*Glass door*	98	33	244	85	5.3	18
3	Anti-panic door	246	91	124	39	11.9	24
4	*Wood door-2*	67	25	144	54	12.7	28
5	Metal door	114	48	200	213	11.9	23
6	*Wood door*	200	80	350	546	15.0	26
7	Metal door with glass spyhole	204	82	280	62	8.0	21
8	*Wood door with glass window*	421	145	170	60	8.5	19

Table 1.
Features of testing environment.

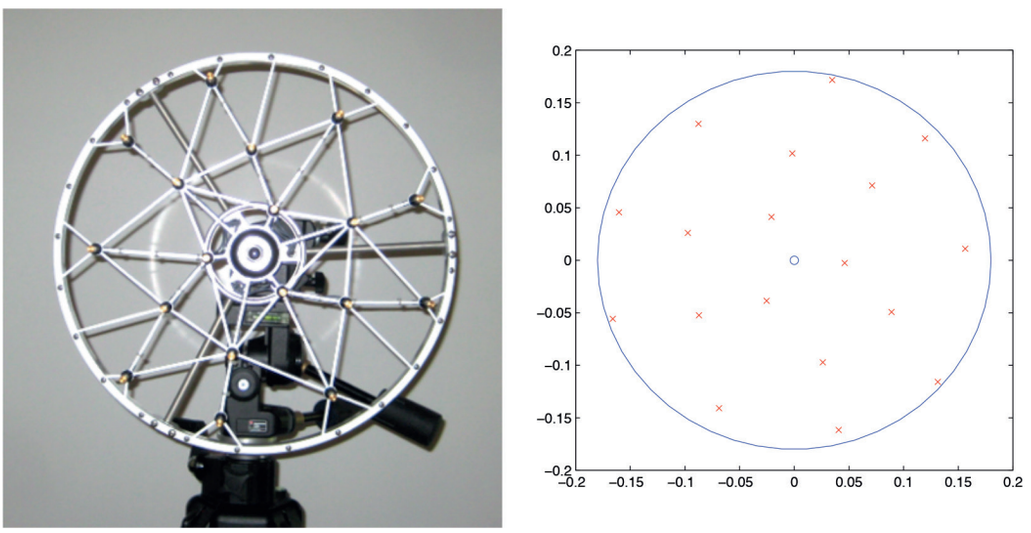

Figure 2.
Left, 18-microphone slice wheel array. Right, microphone positions (dimensions are given in meters).

The post-processed calculations with the reference signals were as follow:

- Without reference signals in the calculations (only in the beamforming case)
- Reference with the central microphone of the array
- Reference with three ½" microphones in the array plane along a diagonal line across the assessed surface: top left, center, and bottom right
- One accelerometer at the surface center in homogeneous elements or two accelerometers centered on the center of each material/surface for elements made of two different materials (e.g., wooden door with glass window—for instance **Figure 1**, Id. 8).

The best results were obtained in beamforming measurements without using references at all and using the central microphone of the array or accelerometers located in areas with different materials in SONAH measurements.

Figure 3.
Example of the beamforming measurement layout.

As the amount of data collected is very large, only the results for the base partition element and a typical and representative example for one of the doors (anti-panic door, **Figure 1**; Id. 3) are exposed. The remaining elements under study were treated in a similar way.

In order to compare the results obtained with those from a standardized technique, the partition elements under test were also measured using the intensity standard described in ISO 15186-2 [2]. The configuration of the emitting room was the same than in the array-based measurements. In the receiving room, measurement grids with at least one point every 30 cm in horizontal and 40 cm in vertical were defined, carrying out two measurement sequences and averaging in each measurement point the intensity obtained for both measurements. Twenty-second measurements were taken in each measurement point using the 12-mm separator, which make possible the measure in a frequency range from the third octave band centered on 200 Hz to the one centered on 5 kHz. Moreover, the calculation of field indicators (F_2, F_3, F_4) according to ISO 9614-1 [3] was performed to evaluate the accuracy of the measurements. Favorable results were obtained for the engineering degree of accuracy in all the cases.

The base partition element consists of a laminated plasterboard wall built on metal profiles. Even though there are other eligible elements such as brick or plaster walls, the laminated plasterboard wall is proposed as a base reference due to the extensive bibliography available for such element [28]. In addition, this element is

Figure 4.
Example of the SONAH measurement layout.

frequently used either independently or combined with doors as partition solutions, forming vertical walls between rooms.

Figure 5 shows the results through intensity and beamforming for the whole wall and through SONAH in three points of the wall in the third octave band. It can be observed, in the three images, that the wall is homogeneous separating element without leaks and, as a consequence, the intensity and pressure maps are uniform over all the surface of the element without leakages or fissures.

In the case of the anti-panic door, **Figure 6** shows the results obtained. **Figure 6(a)** shows the graphical results obtained from the sound intensity measurements (the upper-left point should not be considered because a measurement error took place). Analyzing the results obtained, it is possible to observe that the door exhibits a very homogeneous behavior with very little differences in sound intensity transmission and in addition in the sound insulation. Taken into account that, according to the intensity standard ISO-15186-2 [2], it is not possible to expand the measurement grid until the floor, it was not possible to identify the leakage in the bottom part of the door because the measurement grid does not cover this part.

The sound pressure maps obtained with beamforming and SONAH are those shown in **Figure 6(b)** and **(c)**, where it is possible to observe the areas where there is a higher sound pressure level emitted, in other words, the areas with the lower sound insulation. This area is located at the bottom of the door, because there is no adjustment between the door and the floor. The rest of the door exhibits a very homogeneous behavior because there is a big difference in sound pressure level among the main noise source and the rest ones.

a)

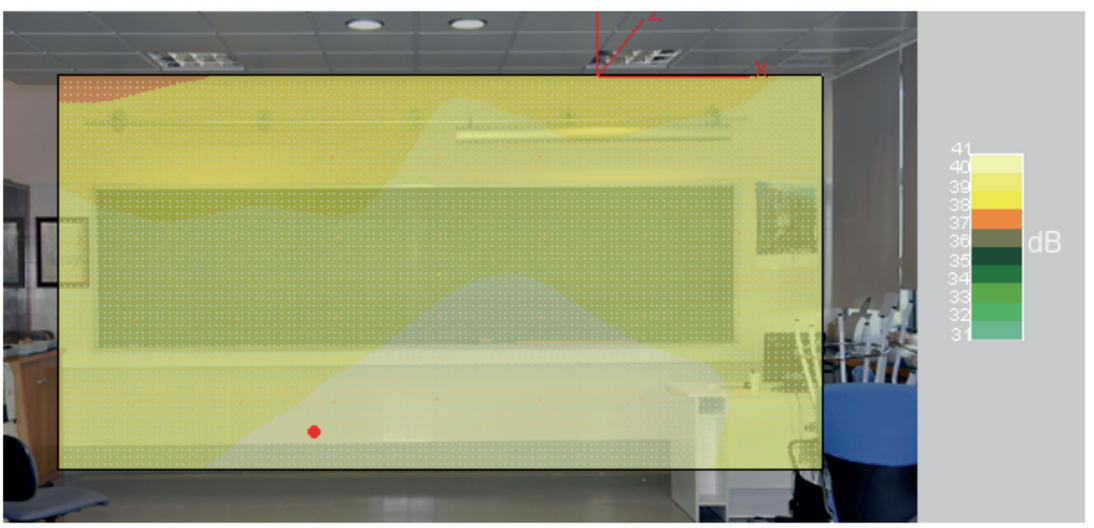

b)

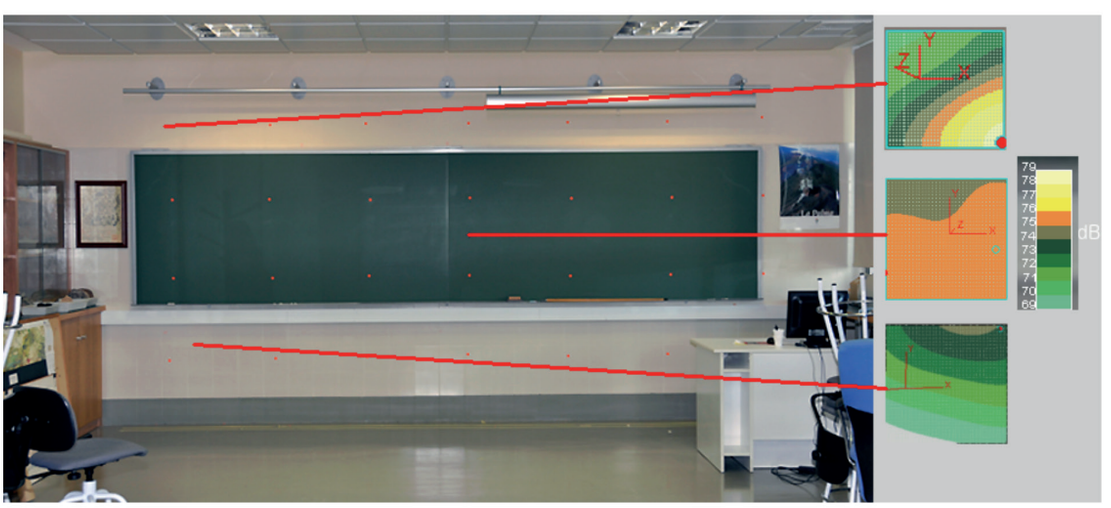

c)

Figure 5.
Results obtained for the base element. (a) Intensity map (200–5 kHz). (b) Pressure map with Beamforming (1-5 kHz) with 10 dB dynamic range. (c) Pressure map with SONAH (160-1600 Hz) with 10 dB dynamic range.

Figure 6.
Results obtained for the anti-panic door. (a) Sound intensity map (200–5 kHz), (b) pressure map with beamforming (1–5 kHz) with 10 dB dynamic range, and (c) pressure map with SONAH in the door center (160–1600 Hz) with 10 dB dynamic range.

If both measurements are compared, the results show a similar behavior, but intensity measurements do not identify the leakage at the bottom part of the door due to the measurement grid chosen.

3. Conclusions

The sound pressure technique based on ISO 16283-1 regulation only requires an analyzer with a third-of-an-octave accuracy, both in sound pressure level and reverberation time readings. In order to apply the measurement technique based on ISO 15186-2, however, it is necessary to use an intensity probe kit in conjunction with a two-channel analyzer with higher sensitivity than that required for sound pressure measurements. Beamforming and SONAH techniques require complex and costly sound instrumentation if compared with that commonly used for in situ assessment of airborne sound insulation, whether by pressure or intensity techniques; this is due to the large number of channels required, the application of processing algorithms with high computational cost and to the design, and preparation of specific microphone arrays.

Although beamforming and SONAH techniques are usually successfully applied in free-field conditions, the use of these techniques under different conditions pinpoints those areas with higher sound transmission. The joint use of beamforming and SONAH techniques on the construction elements under study quickly allows to identify areas of maximum sound transmission on the constructive element under test. In addition, whereas the setting up and the verification of the measurement system based on beamforming and SONAH are initially a time-consuming task, subsequent measurements are carried out in less time than that needed for pressure and intensity techniques, resulting in a greater repeatability of the test and therefore with less influence of potential sound field variations during the in situ measurement.

In beamforming technique applications, the best results are obtained without reference signals, while in SONAH technique are obtained using the reference from accelerometer signals or from the central microphone of the array. The use of alternative processing algorithms in beamforming would allow greater detail and definition on the identification of different sound transmission areas through the partition element.

In conclusion, the implementation of a measurement system based on the combined use of beamforming and SONAH techniques identifies in an accurate way

leakages and weakened areas of partition elements under test. This working model allows to analyze quickly and effectively the behavior of acoustic insulation in areas where there are leaks or weakenings of the partition elements since, once configured the instrumentation system, it is only necessary to perform one measure at each application distance of the corresponding technique to obtain a first estimation of the partition element sound insulation quality.

Acknowledgements

This methodology was developed and granted by the project "Determination of the acoustic insulation of solid, acoustic and fire-resistant doors" (JCCM, Ref. PPII10-0172-426).

The publication of this chapter was funded by Escuela Politécnica de Cuenca - UCLM.

Author details

José A. Ballesteros*, Samuel Quintana and Marcos D. Fernandez
Escuela Politécnica de Cuenca, Universidad de Castilla-La Mancha, Cuenca, Spain

*Address all correspondence to: josea.ballesteros@uclm.es

References

[1] International Organization for Standardization, ISO 16283-1:2015. Acoustics–Field Measurement of Sound Insulation in Buildings and of Building Elements—Part 1: Airborne Sound Insulation; 2015

[2] International Organization for Standardization, ISO 15186-2:2003. Acoustics. Measurement of Sound Insulation in Buildings and of Building Elements Using Sound Intensity. Part 2: Field Measurements; 2003

[3] International Organization for Standardization, ISO 9614-1:1993. Acoustics-Determination of Sound Power Levels of Noise Sources Using Sound Intensity—Part 1: Measurement at Discrete Points; 1993

[4] Ballesteros JA, Quintana S, Fernández MD, Martínez L. Application of beamforming and SONAH to airborne noise insulation measurements. In: Berlin Beamforming Conference; 2012

[5] Johnson DH, Dudgeon DE. Array Signal Processing: Concepts and Techniques. Englewood Cliffs: PTR Prentice Hall; 1993: pp. 1-523

[6] Hald J. Basic theory and properties of statistically optimized near-field acoustical holography. The Journal of the Acoustical Society of America. 2009;**125**:2105-2120

[7] Lafon B, Antoni J, Sidahmed M, Polac L. Cyclic sound intensity and source separation from nah measurements on a diesel engine. Journal of the Acoustical Society of America. 2008;**123**(5):3387

[8] Gerges SN, Fonseca WD, Dougherty RP. State of the art beamforming software and hardware for applications. In: Proceedings of the 16th International Congress on Sound and Vibration; 2009

[9] Nordborg A, Wedemann J, Willenbrink L. Optimum array microphone configuration. In: INTER-NOISE and NOISE-CON Congress and Conference Proceedings, no. 6, Institute of Noise Control Engineering; 2000. pp. 2318-2323

[10] Marroquin M. A comparison of seven different noise identification techniques. SAE Transactions. 2003;**112**(6):2141-2151

[11] Hald J, Christensen J. A class of optimal broadband phased array geometries designed for easy construction. In: INTER-NOISE and NOISECON Congress and Conference Proceedings, no. 3, Institute of Noise Control Engineering; 2002. pp. 1993-1998

[12] Christensen J, Hald J. Technical Review, Beamforming, B&K Technical Review 1; 2004

[13] Ginn K, Hald J. Combined NAH and beamforming using the same microphone array. In: Forum Acusticum; 2005

[14] Ginn K, Hald J, Gade S. STSF-Practical instrumentation and application. Digital filter analysis: Real-time and non real-time performance. B & K Technical Review. 1989;**2**:21-27

[15] Capon J. High-resolution frequency-wave number spectrum analysis. Proceedings of the IEEE. 1969;**57**(8):1408-1418

[16] Sijtsma P. Clean based on spatial source coherence. International Journal of Aeroacoustics. 2007;**6**(4):357-374

[17] Brooks TF, Humphreys WM. A deconvolution approach for the mapping of acoustic sources (DAMAS) determined from phased microphone

arrays. Journal of Sound and Vibration. 2006;**294**(4):856-879

[18] Sarradj E, C Schulze C, Zeibig A. Identification of Noise Source Mechanisms Using Orthogonal Beamforming. Noise and Vibration: Emerging Methods; 2005

[19] Schmidt R. Multiple emitter location and signal parameter estimation. IEEE Transactions on Antennas and Propagation. 1986;**34**(3):276-280

[20] Sarradj E. A fast signal subspace approach for the determination of absolute levels from phased microphone array measurements. Journal of Sound and Vibration. 2010;**329**(9):1553-1569

[21] Hald J. Patch near-field acoustical holography using a new statistically optimal method. B & K Technical Review. 2003;**1**:40-50

[22] Dirks G, Gade S, Hald J, The use of near field acoustical holography for leak. In: INTER-NOISE and NOISE-CON Congress and Conference Proceedings, Institute of Noise Control Engineering; 2005

[23] Instituto Eduardo Torroja de ciencias de la construcción (Eduardo Torroja Institute for Building Sciences), Código Técnico de la Edificación-CTE; Catálogo de elementos constructivos del CTE (Technical Code for Building-CTE; Catalogue of building elements of the CTE); 2010

[24] Asociación Española de Normalización (Spanish Association for Normalization), UNE-EN 12354-1:2000. Estimación de las características acústicas de las edificaciones a partir de las características de sus elementos. Parte 1: Aislamiento acústico del ruido aéreo entre recintos. (Estimation of the acoustic characteristics of buildings from the characteristics of their elements part 1: Airborne sound isolation between rooms); 2000

[25] Brüel & Kjaer. LAN-XI data acquisition hardware for PULSE and test for I-deas. Brüel & Kjaer Product Data. 2016:1-40

[26] Brüel & Kjaer, PULSETM Array-based Noise Source Identification Solutions: Beamforming Type 8608, Acoustic Holography Type 8607 and Spherical Beamforming Type 8606, Brüel & Kjaer Product Data 1-12; 2013

[27] Jacobsen F, Tiana-Roig E. Measurement of the sound power incident on the walls of a reverberation room with near field acoustic holography. Acta Acustica United with Acustica. 2010;**96**(1):76-81

[28] Ortí JS, Galiana JL, Martínez AU. Aislamiento acústico de particiones ligeras multicapa: estudio del material absorbente y del sistema de montaje (Sound isolation of light multilayer partitions: Study of the absorbent materials and the assembly system). Universidad Politécnica de Valencia; 2003